

Direct Glucose Sensing In the Physiological Range Through Plasmonic Nanoparticle Formation

Sarah Unser, Ian Campbell, Debrina Jana, Laura Sagle*

Without Interfering Agents



With Interfering Agents



Figure S1. Reaction with 0.2 mM HAuCl_4 was carried out in the presence of no glucose, both with and without interfering agents present. No reaction is observed for the sample over the course of three hours.

Direct Glucose Sensing In the Physiological Range Through Plasmonic Nanoparticle Formation

Sarah Unser, Ian Campbell, Debrina Jana, Laura Sagle*

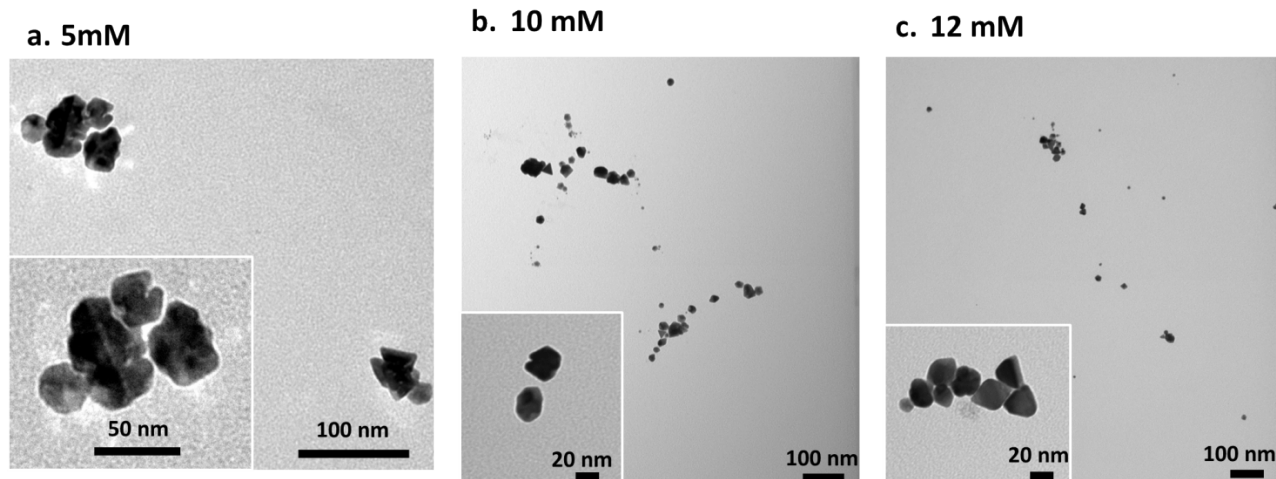


Figure S2. TEM images of nanoparticles formed at varying concentrations of glucose not shown in **Figure 4**.

Direct Glucose Sensing In the Physiological Range Through Plasmonic Nanoparticle Formation

Sarah Unser, Ian Campbell, Debrina Jana, Laura Sagle*

Glucose Concentration (mM)	Time Elapsed (seconds)	Standard Deviation	Glucose Concentration (mM)	Rate Constant, k (sec ⁻ⁿ)	Critical Growth Exponent, n
1.25	421.5	± 63.8	1.25	$1.7 \pm 8.7 \times 10^{-14}$	5.3 + 0.208
1.50	289.1	± 49.4	2	$9.7 \pm 3.5 \times 10^{-15}$	5.5 + 0.356
2	267.8	± 83.6	7	$1.3 \pm 1.9 \times 10^{-6}$	4.9 + 0.000
3	65.1	± 3.8	12	$4.7 \pm 3.4 \times 10^{-7}$	4.9 + 0.007
5	37.9	± 9.4	15	$4.4 \pm 2.3 \times 10^{-6}$	4.9 + 0.013
7	22.5	± 14.1	18	$1.9 \pm 3.0 \times 10^{-5}$	4.9 + 0.050
10	23.3	± 0.3			
12	30.7	± 4.6			
15	12.9	± 4.3			
18	14.2	± 1.9			
20	11.3	± 5.6			
50	9.8	± 3.9			

Table S3 and S4. **Table S3** displays nanoparticle formation times with increasing glucose concentrations, left. As the concentration of glucose increases, the time for formation decreases. **Table S4** displays the rate constants and critical growth exponent from fitting the data to the Avrami Model, for concentrations not shown in **Table 1**, right.

Direct Glucose Sensing In the Physiological Range Through Plasmonic Nanoparticle Formation

Sarah Unser, Ian Campbell, Debrina Jana, Laura Sagle*

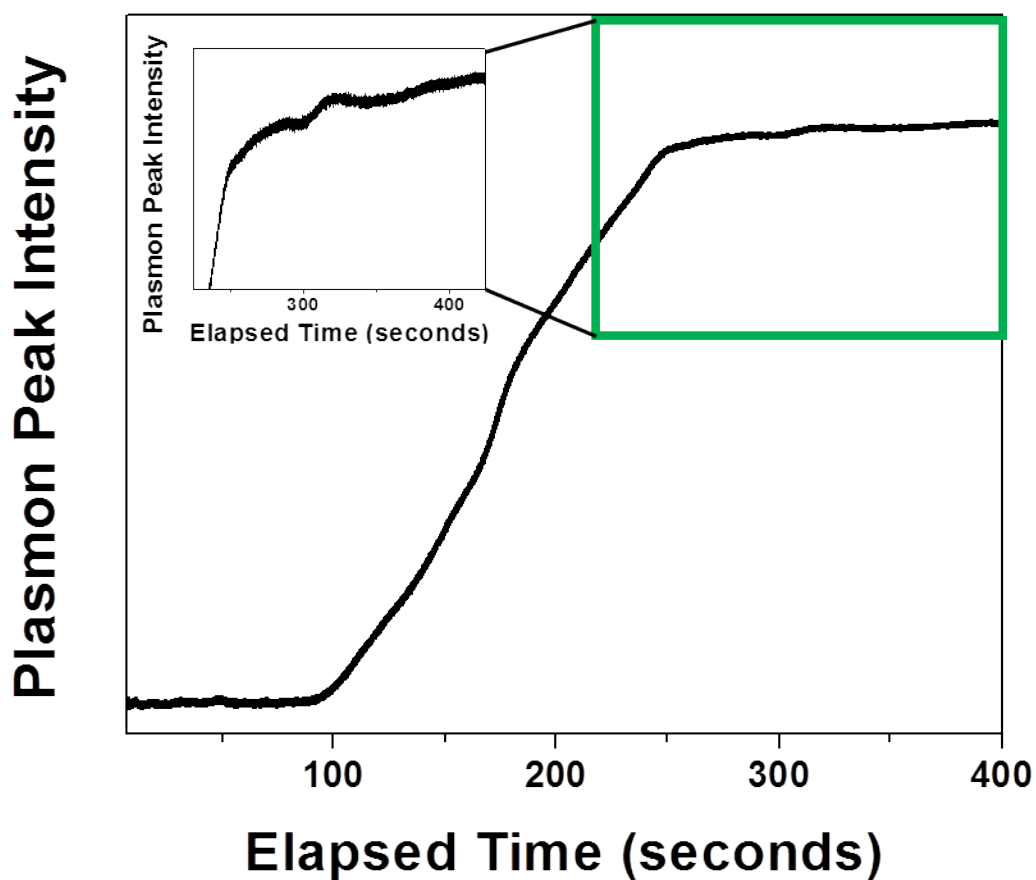


Figure S4. Nanoparticle growth from a gold salt precursor in the presence of 1.5 mM glucose exhibits mainly a sigmoidal trend indicative of nucleation and aggregative growth. After the sigmoid has completed a small upward trend is visualized around 220 seconds which indicates some Ostwald ripening.

Direct Glucose Sensing In the Physiological Range Through Plasmonic Nanoparticle Formation

Sarah Unser, Ian Campbell, Debrina Jana, Laura Sagle*

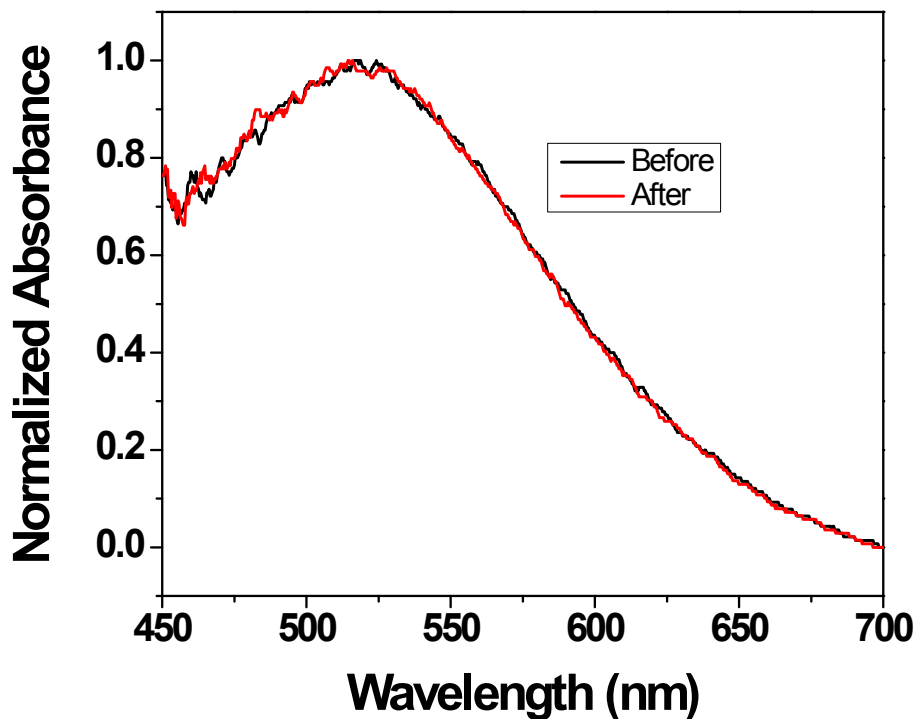


Figure S5. The UV-visible spectrum shows the hole mask colloidal lithography sample before and after the addition of 50 mM HEPES to the substrates. No change in UV-Visible spectrum is detected.

Direct Glucose Sensing In the Physiological Range Through Plasmonic Nanoparticle Formation

Sarah Unser, Ian Campbell, Debrina Jana, Laura Sagle*

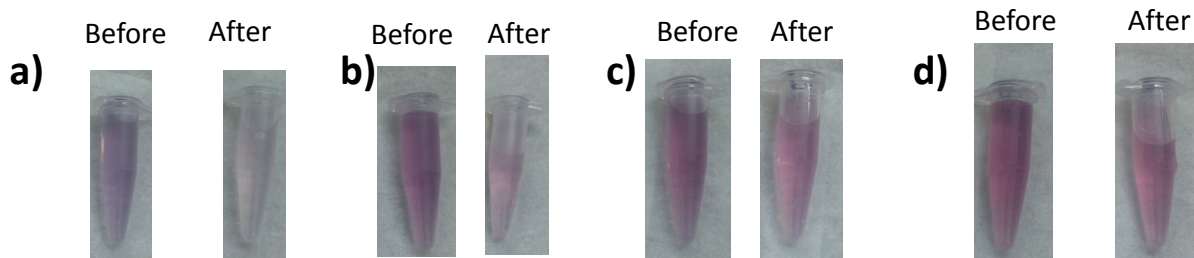


Figure S6. The above images show nanoparticles that have been formed with increasing concentrations of glucose, a) 3 mM glucose, b) 7 mM glucose, c) 10 mM glucose, and d) 20 mM glucose, before and after they have been filtered through 0.1 μm filters. The lower the concentration of glucose, the larger the resulting nanoparticles that form are. This is demonstrated by a loss in intensity, **Figure 6**, in lower concentrations of glucose whose large nanoparticles become trapped in the pores of the filter. At higher concentrations of glucose such as 10 mM and 20 mM the drop in intensity is less apparent due to the formation of smaller nanoparticles, <20 nm, that can easily pass through the 0.1 μm filters.

Direct Glucose Sensing In the Physiological Range Through Plasmonic Nanoparticle Formation

Sarah Unser, Ian Campbell, Debrina Jana, Laura Sagle*

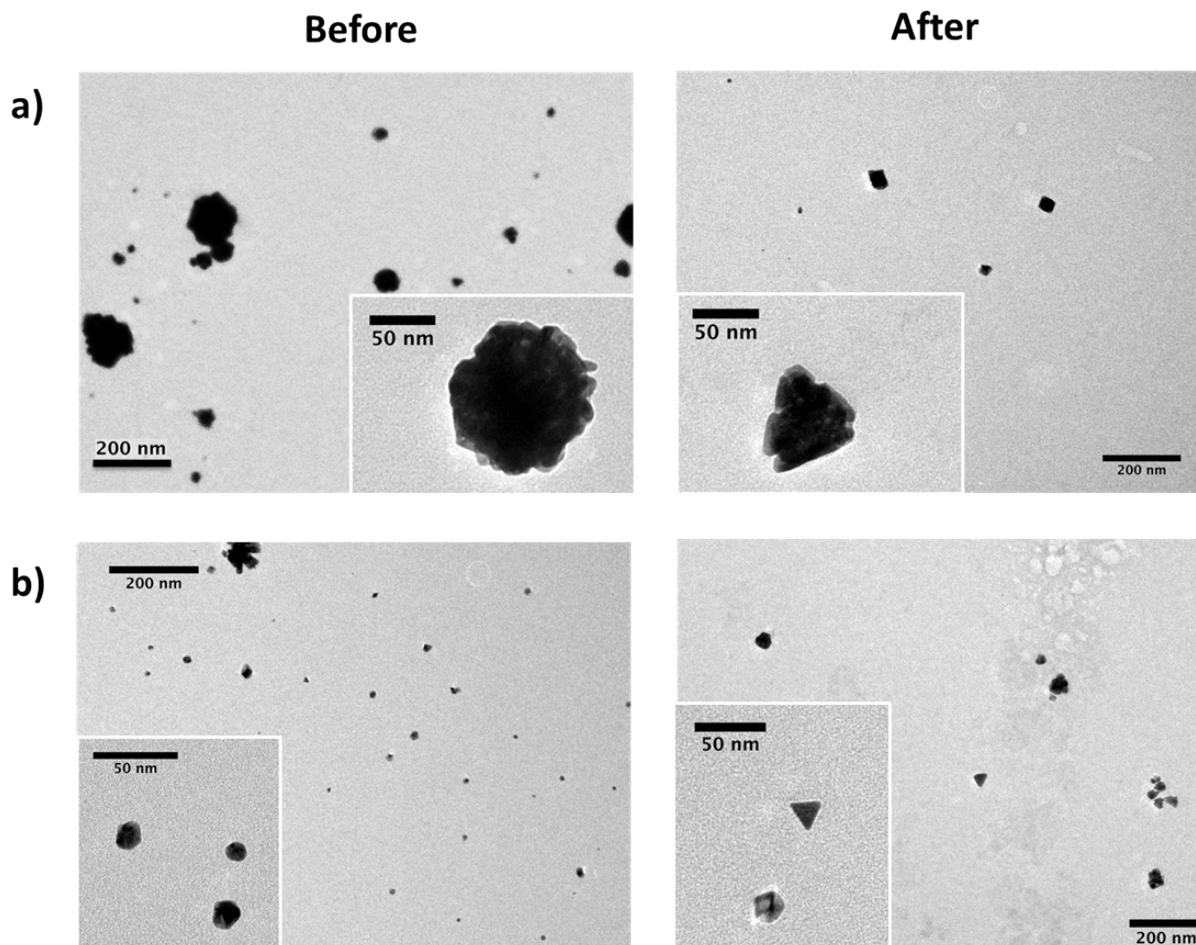


Figure S7. The above TEM images correspond with samples before and after filtration of solutions relating to the images in **Figure S6**. At low glucose concentrations a) There is a wide distribution of nanoparticle size above and below 100 nm before filtration, but after filtration the size of the nanoparticles is controlled under 100 nm while b) 20 mM glucose formed particles show a much narrower range of distribution with mainly particles below 100 nm, therefore less of a noticeable difference is visualized in both the TEM image above and in color, **Figure S6**.

Direct Glucose Sensing In the Physiological Range Through Plasmonic Nanoparticle Formation

Sarah Unser, Ian Campbell, Debrina Jana, Laura Sagle*

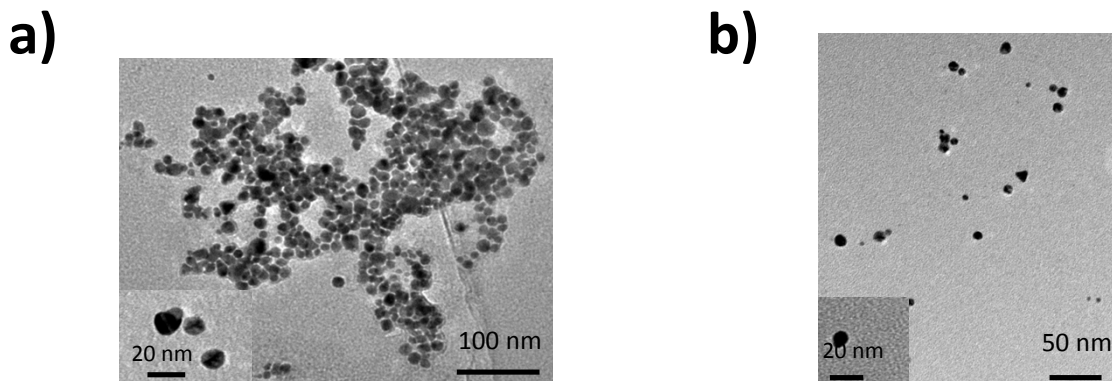


Figure S8. The TEM image displays nanoparticle formation of a) 50 mM glucose and b) 50 mM glucose along with interfering agents. It is apparent that nanoparticle size at this concentration is larger for the sample without interfering agent, which is also consistent with the plot shown in **Figure 7**.

Direct Glucose Sensing In the Physiological Range Through Plasmonic Nanoparticle Formation

Sarah Unser, Ian Campbell, Debrina Jana, Laura Sagle*

a)			b)		
Peaks			Peaks		
Diameter(μm)	Volume %	Width	Diameter(μm)	Volume %	Width
0.1019	23.90	0.0894	0.1071	28.60	0.0765
0.0335	76.10	0.0218	0.0153	71.40	0.0074

Figure S9. Nanoparticles formed were further analyzed through dynamic light scattering measurements. Nanoparticles were diluted by half using 50 mM HEPES buffer pH 7. The solution was then added to the sample chamber of the Microtrac Zetatrak particle size analyzer. Table a) shows from 50 mM glucose and b) 50 mM glucose + interfering agents. The particle size decreases in the presence of glucose and interfering agents which can be distinguished by the difference in color (**Fig. 7b**).

Direct Glucose Sensing In the Physiological Range Through Plasmonic Nanoparticle Formation

Sarah Unser, Ian Campbell, Debrina Jana, Laura Sagle*

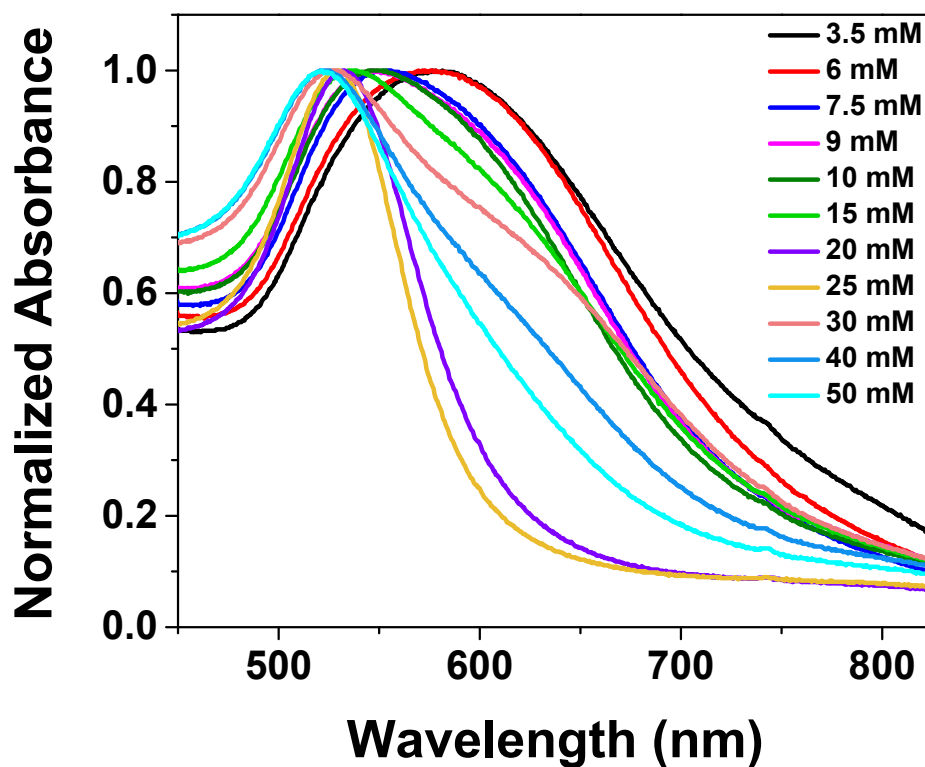


Figure S10. The UV-Visible spectra shows the shift in plasmon peak in the presence of both glucose and interfering agents. With increasing concentrations of glucose, the UV-Visible peak becomes more defined that can also be detected optically by a color change from dark blue/purple to a pink/red color, as shown in **Figure 7b**.

Direct Glucose Sensing In the Physiological Range Through Plasmonic Nanoparticle Formation

Sarah Unser, Ian Campbell, Debrina Jana, Laura Sagle*

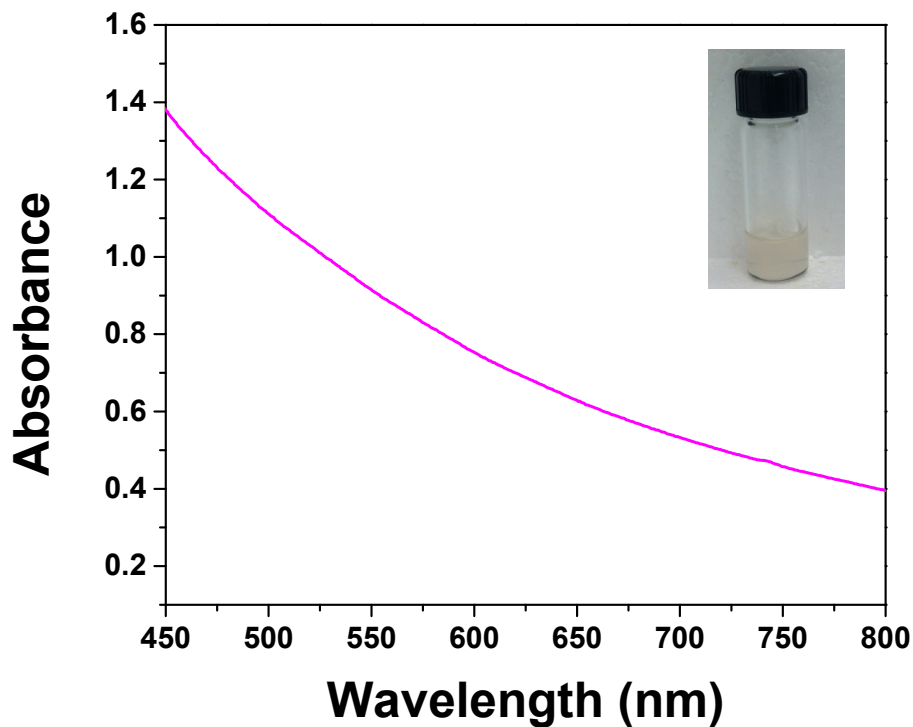
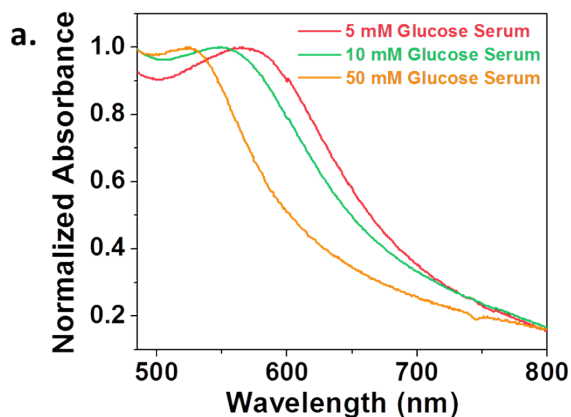


Figure S11. The UV-visible spectrum of 20% mouse serum shows no distinct peak. This indicates that the peak that is seen with glucose is a product of the reduction of gold salt precursor.

Direct Glucose Sensing In the Physiological Range Through Plasmonic Nanoparticle Formation

Sarah Unser, Ian Campbell, Debrina Jana, Laura Sagle*



b.

Glucose Concentration (mM)	Plasmon Peak with Interfering Agents (nm)	Plasmon Peak in Serum (nm)
5	567.00	561.00
10	546.00	543.00
50	521.50	520.50

Figure S12. Nanoparticles formed in serum samples were characterized by UV-visible spectroscopy showing their plasmon peaks at a) 5 mM, 10 mM, and 50 mM glucose, and b) their corresponding plasmon peaks are compared against the plasmon peaks against interfering agents.

Direct Glucose Sensing In the Physiological Range Through Plasmonic Nanoparticle Formation

Sarah Unser, Ian Campbell, Debrina Jana, Laura Sagle*

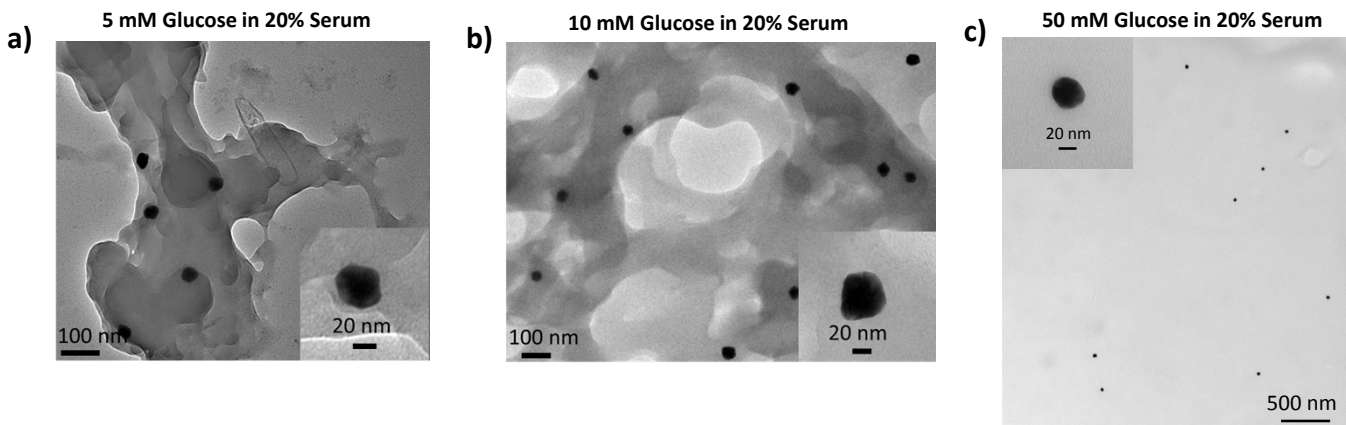


Figure S13. Nanoparticles formed in serum samples were characterized by TEM resulting in the images a) 5 mM glucose, b) 10 mM glucose and c) 50 mM glucose. Similar to the samples without serum, the size of the particles decreases with increasing glucose.

Direct Glucose Sensing In the Physiological Range Through Plasmonic Nanoparticle Formation

Sarah Unser, Ian Campbell, Debrina Jana, Laura Sagle*

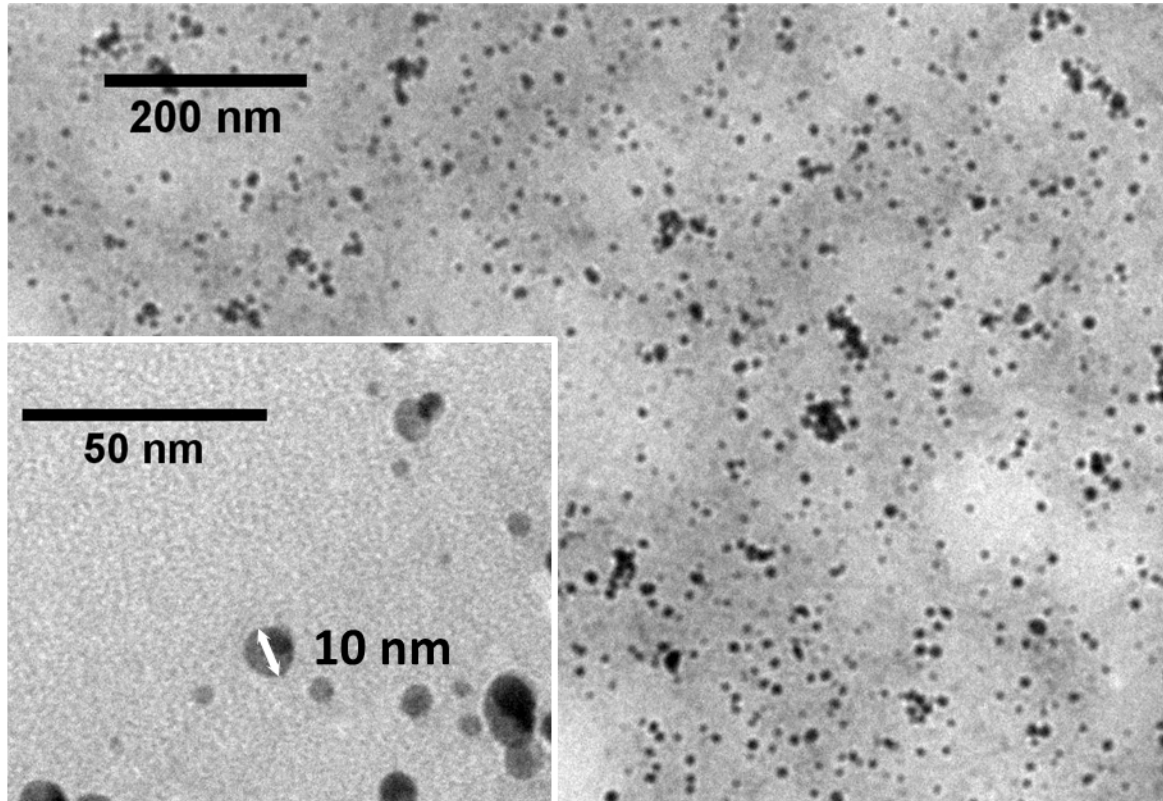


Figure S14. Nanoparticles formed in bovine urine in the presence of 50 mM glucose.